PHYSICAL REVIEW B VOLUME 61, NUMBER 16 15 APRIL 2000-II

Tuning the insulator−quantum Hall liquid transitions in a two-dimensional electron gas using self-assembled InAs

G. H. Kim, J. T. Nicholls, S. I. Khondaker, I. Farrer, and D. A. Ritchie
Cavendish Laboratory, Madingley Road, Cambridge, CB3 OHE, United Kingdom
(Received 29 November 1999)

We investigate the transport properties of two-dimensional electron gases (2DEG's) formed in a $GaAs/Al_{0.33}Ga_{0.67}As$ quantum well, where InAs has been inserted into the center of the GaAs well. Depending on the growth conditions, the InAs forms either self-assembled quantum dots or dashes, and due to the resulting strain fields repulsive short-range scattering is experienced by the conduction electrons in the 2DEG. In a perpendicular magnetic field there are transitions between quantum Hall liquids at filling factors $\nu=1$ and $\nu=2$ and the insulating phase. Depending on the amount of InAs coverage, the degree of disorder in the 2DEG can be varied, changing the relative size of the $\nu=1$ and $\nu=2$ regions in the disorder–magnetic-field phase diagrams. Thermal studies show a spin gap at filling factor $\nu=1$, which collapses as the magnetic field is decreased. Microscopic information about the dots was obtained from structural characterization, as well as from conductance measurements through individual dots isolated using a submicron split gate.

In a perpendicular magnetic field a two-dimensional electron gas (2DEG) at low temperatures exhibits the quantum Hall (QH) effect. In a strong magnetic field there are Landau levels (LL's), and the picture of extended states at the LL centers and localized states between LL's provides a simple description of the quantum Hall effect. When the magnetic field (B) is decreased at fixed carrier density n, the localized and extended states move down in energy and alternately pass through the Fermi energy. When the Fermi energy passes through the extended states, both ρ_{xx} and ρ_{xy} vary smoothly. In contrast, when the Fermi energy is between LL's and pinned in the localized states, the transverse resistivity ρ_{xy} is quantized, and the longitudinal resistivity $\rho_{xx} \rightarrow 0$ as the temperature is reduced to zero.

From scaling arguments it is believed that there are only weakly localized states in a noninteracting 2DEG at low temperatures and zero magnetic field. After the discovery of the quantum Hall effect it was realized by Khmelnitskii[1] and Laughlin[2] that to be consistent with scaling theory the extended states at the center of each LL could rise up in energy as the magnetic field is reduced. An alternative to this floating-up picture is that the extended states somehow disappear at a finite magnetic field. The issue of whether there is floating or not resurfaced when measurements[3–5] of disordered 2DEG's in GaAs showed that with increasing B, there is a transition from a strongly localized insulating zero-field phase, to a QH liquid of filling factor $\nu=nh/eB=2$. When the magnetic field is increased further, there is a transition back to the insulating phase. The lower field transition, the insulator $\rightarrow \nu=2$ QH liquid transition, supports the floating-up picture, and the phase diagram constructed in n-B space from the measured[5] 0-2-0 transitions looks similar to the global diagram proposed by Kivelson *et al.*[6] Later measurements[7] of high-mobility GaAs samples taken to low carrier densities showed transitions from an insulator $\rightarrow \nu=2$ QH liquid $\rightarrow \nu=1$ QH liquid→insulator (0-2-1-0) as B was increased, and *not* the 0-1-2-1-0 sequence of transitions expected if each spin-split LL were to float up independently. Transitions through the $\nu=1$ QH liquid have also been observed[8,9] in 2D SiGe hole gases, where the ratio of the Zeeman energy to the LL energy spacing is greater than in GaAs. The nature of the QH insulator-liquid transitions continues to be an area of interest,[10] and the floating up of LL's is thought to be relevant to recent measurements of a 2D "metal-insulator" transition.

In this paper we present a different GaAs system for observing insulator-QH transitions, where the scattering in the 2DEG can to some extent be tuned by self-assembled InAs structures that are grown in the center of the GaAs quantum well. Depending on the amount of InAs deposited, it is found that the degree of spin splitting varies, changing the shape of the experimental n-B diagram. Previous studies[11] of InAs quantum dots grown in the vicinity (150–800 Å) of a 2DEG, show that a dot-induced modulation of the 2D potential dramatically reduces the transport mobility. Using a split gate to isolate individual dots in samples where InAs dots were deposited approximately 200 Å below the 2DEG, thermal studies of the conductance claim[12] the electron confinement energy can be as large as 14 meV. Studies of InAs dots placed even closer to the 2DEG have been carried out by Yoh *et al.*,[13] who were able to measure some charging effects. Later, the scattering introduced by dots grown 30 Å from the $Al_xGa_{1-x}As/GaAs$ heterointerface was investigated,[14] and it was shown how self-assembled InAs dots can tailor the electrical properties of a 2DEG. In this study a similar approach has been used to vary the scattering in what would otherwise be a high-mobility ($\mu > 10^5$ cm^2/V s) 2DEG. Preliminary measurements in the QH regime have been presented elsewhere.[15]

The synthesis and characterization of the samples are described in Sec. I. Section II A describes the mesoscopic transport properties of individual quantum dots formed by the self-assembled InAs structures. The macroscopic transport properties of the samples, in the QH regime, are presented in Sec. II B. A discussion of all the results is given in Sec. III.

I. SAMPLES: SYNTHESIS AND STRUCTURAL CHARACTERIZATION

Measurements are presented for samples from five different wafers, all of which have the basic structure shown in

0163-1829/2000/61(16)/10910(7)/$15.00 PRB 61 10 910 ©2000 The American Physical Society

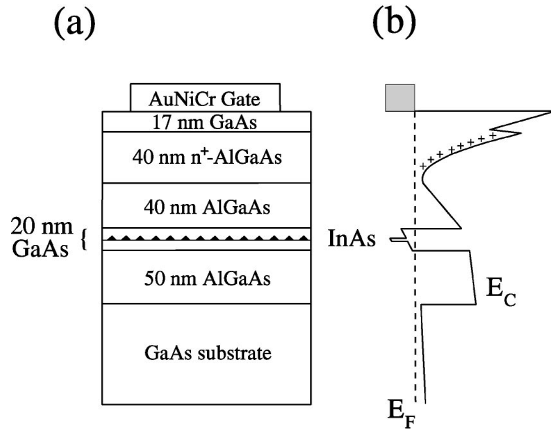

FIG. 1. (a) Structure of the samples. (b) Schematic of the conduction-band profile in the growth (z) direction, at the site of InAs deposition.

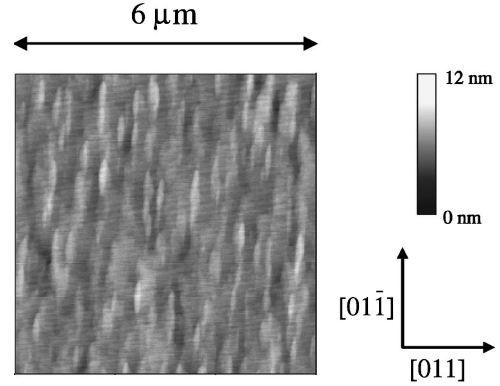

FIG. 2. A 6 μm$\times$6 μm AFM image of a sample grown in a similar fashion to sample C, but with a growth interruption and capping. Dashes, approximately 5000$\times$600 Å^2, are aligned in the [01$\bar{1}$] direction.

Fig. 1(a), but with slightly different properties, as listed in Table I. The samples were grown by molecular-beam epitaxy on (100) GaAs substrates and consist of a 200-Å-wide GaAs/$Al_{0.33}Ga_{0.66}As$ quantum well that is modulation doped on one side using a 400-Å spacer layer. The growth of the GaAs quantum well was interrupted at its center, and the wafer was cooled from 580 °C to 525 °C. The shutter over the indium cell was opened for 0, 60, and 80 sec, allowing growth of 0, 1.61, and 2.15 ML of InAs, respectively. A cap layer of GaAs was grown at 530 °C, before the substrate temperature was raised to 580 °C for the remainder of the growth.

The thickness of the GaAs capping layer over the InAs determines the dimensions and shape of the InAs structures.[16,17] In sample A, the 2.15 ML of InAs were capped by a 50-Å GaAs layer, and self-assembled InAs quantum dots were formed. A transmission electron microscope (TEM) image taken from the same wafer as sample A has been presented as sample 2 in Ref. 17; the dots have a density of 3×10^{9} cm^{-2}, and are typically 280 Å in diameter and 40 Å in height. In sample C, 2.16 ML of indium were covered with a 10 Å GaAs capping layer, and dashes of typical dimensions $\sim$5000$\times$600 Å^2 were formed; these are elongated in the [01$\bar{1}$] direction, as shown in the atomic force microscope image in Fig. 2. In sample B, 1.61 ML of InAs were capped with 10 Å of GaAs and dashes similar to those shown in Fig. 2 were formed. Sample D was grown with 1 ML of InAs, which was capped by 10 Å of GaAs; this sample contains one continuous layer of InAs, being below the critical coverage required for the onset of Stranski-Krastinow growth. Wafer E is a control sample where the growth was interrupted at the center of the GaAs quantum well, but the indium shutter was not opened. In samples B and C there is insufficient strain for the InAs dashes to be visible using TEM.[17]

The as-grown carrier densities of the 2DEG's are typically $n=1.5$–2.5×10^{11}cm^{-2}, and can be varied by the voltage V_g applied to a AuNiCr gate that is evaporated on the sample surface, approximately 1000 Å above the quantum well [see Fig. 1(a)]. Figure 3 shows the low-temperature mobilities of the five samples as a function of carrier density n; μ was determined from the zero-field resistivity, and n from the Hall slope at low magnetic fields. Compared to the control sample (E) the addition of InAs reduces the 2DEG mobility μ by up to an order of magnitude. In general, the $\mu-n$ curves follow the relation $\mu\sim n^{\alpha}$, where $\alpha=0.7-0.8$ at high n, typical of modulation-doped samples. With increasing InAs the samples show more pronounced behavior at low n, with $\alpha>0.8$, reflecting the difficulty in screening the InAs structures at these densities. Although samples A and C contain the same amount of indium, the strain in the dot sample (A) causes its low-temperature mobility μ to be lower than that of the dash sample (C). The structural anisotropy of the dash samples is reflected in the mobility, which is twice as large in the [011] direction as in the [01$\bar{1}$] direction. The dot sample (A) shows a similar anisotropy, which reflects the propensity of the dots to line up along the [01$\bar{1}$] direction.[18] For samples A–D, the ratio of the transport to quantum lifetime is approximately five, which is a consequence of short-range scattering from the InAs.[19]

TABLE I. Structural properties of samples. QW represents quantum well.

Sample	InAs coverage (ML)	Capping layer thickness (Å)	Structure
A	2.15	50	dots in a QW
B	1.61	10	dashes in a QW
C	2.15	10	dashes in a QW
D	1		continuous InAs in QW
Control E			growth interruption in QW, no InAs

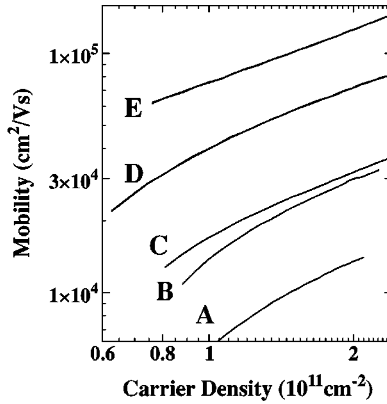

FIG. 3. The low-temperature mobilities (μ) of the samples as a function of carrier density (n) at $T=1.6$ K.

II. TRANSPORT MEASUREMENTS

The wafers were patterned into 800×80 μm^2 Hall bars, and after illumination with a red light-emitting diode, transport measurements were performed in one of two ways. In Sec. II A we present two-terminal conductance measurements through a 1D constriction created by a split gate. We observe Coulomb blockade oscillations through a quantum dot that is in, or close to, the 1D constriction. These conductance measurements provide information about the individual quantum dots[20] formed by the self-assembled InAs structures. In contrast, the quantum Hall measurements described in Sec. II B are sensitive to the repulsive scattering introduced by an ensemble of InAs structures.

A. Split-gate measurements

Electron beam lithography was used to define split gates of length 0.1 μm and gap width of 0.3 μm on the sample surface. In the hope of isolating just one dot the gates are much shorter than those used in ballistic transport measurements.[21] When a negative voltage is applied to the split gate, a short and narrow 1D channel is defined in the 2DEG. Figure 4 shows the conductance characteristics (using an excitation voltage of 0.1 mV) for sample A as a function of the voltage V_{g1} applied to one arm of the split gate, while the other arm is kept fixed at $V_{g2}=-1.67$ V. The traces were measured at 0.3 K, though the conductance peaks could be observed up to 18 K. On different cooldowns, the characteristics were observed at shifted gate voltage positions and were not exactly reproduced. We expect that there is a quantum dot situated in the vicinity of the 1D channel, so that for conductances $G<e^2/h$, transport is dominated by the zero-dimensional properties of the dot. There is a capacitive coupling between the dot and the split gate, and decreasing the gate voltage reduces the numbers of electrons in the dot, giving rise to the Coulomb blockade oscillations shown in Fig. 4.

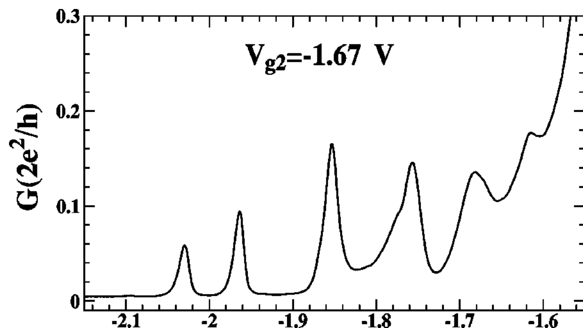

FIG. 4. Conductance characteristics $G(V_{g1})$ of sample A, as a function of the gate voltage V_{g1} applied to one arm of the split gate, while keeping the other arm fixed at $V_{g2}=-1.67$ V.

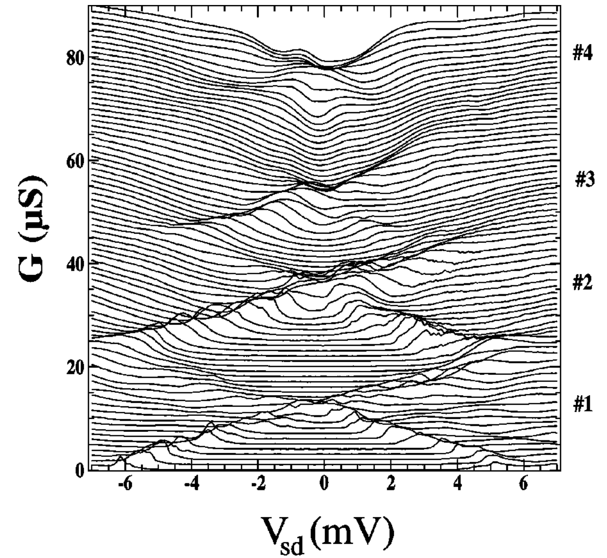

FIG. 5. The nonequilibrium $G(V_{sd})$ characteristics of sample A. The charging energy e^2/C is the energy from the center line to a corner of one of the diamonds. Consecutive sweeps have been offset in the vertical direction by 1 μS. The numbers 1–4 label the last four Coulomb blockade peaks observed in the $G(V_{g1})$ measurements.

Adding a dc source-drain voltage V_{sd} to the ac excitation voltage allows the charging energies e^2/C of the confined electrons to be measured. Figure 5 shows the differential conductance $G=dI/dV_{sd}$ of sample A as the dc source-drain voltage V_{sd} is swept from -7 to $+7$ mV; between each sweep the split-gate voltage V_{sg} is incremented by 5 mV. The diamond-shaped regions of zero conductance are characteristic of Coulomb blockade, and have been observed in deliberately structured quantum dots, as well as in samples where a random background potential causes puddling of electrons.[22] As V_{sg} is made more negative, the number of electrons in the dot decreases and the tunneling barriers become thicker, both of which are responsible for increasing the charging energy e^2/C from 2–3 meV to 6–7 meV. Similar $G(V_{sd})$ characteristics have been measured using split gates deposited over dash samples, but not in the sample (D) where there is a single uniform layer of InAs in the quantum well. This provides strong evidence that in both dot and dash samples the puddling of electrons is caused by strain fields that arise from the 7% lattice mismatch between the InAs and GaAs.

As shown in the schematic conduction-band diagram in Fig. 1(b), there is a narrow and deep InAs well situated in the center of the GaAs quantum well. In the z direction the width of the wave function is determined by the 200-Å-wide GaAs well, which is only weakly perturbed by the InAs. By contrast, in the plane of the 2DEG there are strain fields around

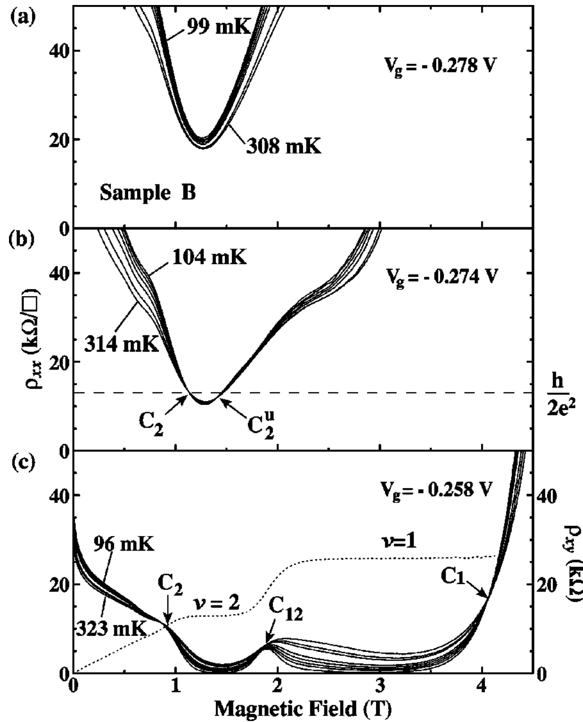

FIG. 6. (a)–(c) The magnetoresistivity $\rho_{xx}(B)$ of sample B for temperatures $T=96$–323 mK for three different gate voltages. The transition points at C_1, C_2, C_{12}, and C_2^u are identified by their temperature independence. The $\rho_{xy}(B)$ trace, shown as a dashed line in (c), was measured at $T=273$ mK.

the dots that are visible[17] in TEM images, and which are expected to affect the conduction-band profile.

The split-gate measurements show that confined electrons exhibit charging effects in both dash and dot samples. The charging energies (≈ 2–3 meV) in dash samples at pinch-off are a factor of 2 smaller than in dot samples, showing that smaller puddles of electrons are confined in dash samples. In both cases an inhomogeneous layer of InAs introduces a disorder potential that localizes the electrons, also altering the properties of the 2DEG in the quantum Hall regime, as described in Sec. II B.

B. Quantum Hall measurements

Four-terminal longitudinal (ρ_{xx}) and transverse (ρ_{xy}) resistivity measurements were performed on Hall bars aligned in the $[01\bar{1}]$ direction, using an excitation current of 2 nA at 14 Hz. The 2D carrier density n was reduced by applying a negative gate voltage V_g to a gate covering the Hall bar. The ability of the electrons to screen out the disorder potential decreases as n is lowered, and therefore V_g can be regarded as a means of varying the effective disorder of the sample, an important parameter in the study of QH transitions.[6]

Figures 6(a)–6(c) show longitudinal magnetoresistivity traces $\rho_{xx}(B)$ for sample B over the temperature range $T=96$–323 mK, for three different gate voltages V_g. As V_g is made more positive, the effective disorder decreases and the zero-field resistivity drops from being greater than 200 kΩ to 30 kΩ. Figure 6(a) shows measurements at $V_g=-0.278$ V, where for all B the resistivity ρ_{xx} increases with decreasing temperature, and hence the sample is always in the insulating phase (0). As in previous studies[5] the temperature independence of $\rho_{xx}(B)$ at a particular magnetic field and gate voltage V_g, is used to identify the boundaries between different QH liquids at $\nu=1$ and 2, and the insulating phase (0). Figure 6(b) shows 0-2-0 transitions at $V_g=-0.274$ V, which are identified by a temperature-independent ρ_{xx} at $B=1.12$ and 1.41 T (labeled C_2 and C_2^u), at which $\rho_{xx}\approx h/2e^2$. At the highest carrier density (lowest disorder), $V_g=-0.258$ V, proper zeros in the low-temperature $\rho_{xx}(B)$ traces have developed at filling factors $\nu=1$ and 2, which are accompanied by QH plateaus in $\rho_{xy}(B)$. The 0-2 transition (C_2) at $B=0.86$ T, and the 1-0 transition (C_1) at 4.05 T are clearly defined because they separate phases of opposite temperature dependence. In contrast, the 1-2 transition (C_{12}) at 1.8 T separates two metallic phases with $d\rho_{xx}/dT>0$, and so this transition is more difficult to identify.

If there are an equal number of positively and negatively charged impurities, the QH plateaus in $\rho_{xy}(B)$ are expected to be centered about the classical value $\rho_{xy}=B/en$. Haug *et al.*[23] showed that when repulsive or attractive scattering centers are deliberately introduced close to a 2DEG, the centers of the QH plateaus are shifted to higher or lower magnetic fields, respectively. The Hall resistivity ρ_{xy} is shown as a dashed line in Fig. 6(c), and the shift of both the $\nu=1$ and 2 plateaus to magnetic fields greater than the classical value show that there is repulsive scattering, as observed by Ribeiro *et al.*[14] A comparison of the upshift of the $\nu=2$ plateaus in samples A and C at similar carrier densities, show there is stronger repulsive scattering in the dot samples (60% upshift) than in the dash samples (16% upshift). In both cases the repulsive scattering increases dramatically as the carrier density is reduced.

Magnetic field sweeps at different temperatures of samples A–C over a range of V_g were used to construct the phase diagrams shown in Fig. 7. The n-B diagrams follow the general trend that, the higher the mobility of the sample, the greater the prominence of the $\nu=1$ quantum Hall liquid phase. Sample C shows a transition from insulating to $\nu=2$ quantum Hall liquid as the magnetic field is increased, and then through $\nu=1$ back to the insulating phase, similar to that observed by Shahar *et al.*[7] The triple point of the phase diagrams shown in Figs. 7(a)–7(c) occurs at $n=3.5$–5.2×10^{10} cm^{-2}, carrier densities that are about three times higher than those of Ref. 7, and approximately five times lower than the samples used in Refs. 3–5. As expected the $\nu=1$ phase is only observed at the lower densities, when the Zeeman energy becomes proportionally stronger compared to the LL spacing.

As mentioned in the context of the mobility, the resistivity $\rho_{xx}(B)$ shows some anisotropy depending on whether the Hall bar is aligned along the $[011]$ or the $[0\bar{1}1]$ direction. Preliminary measurements show that the $n-B$ phase diagrams are unaffected by this anisotropy. Thermal broadening of the LL's may destroy the spin splitting, and there is a question as to whether the temperature independence of ρ_{xx} at a QH transition is appropriate for determining the phase diagrams shown in Fig. 7. To check this we measured the gate voltage positions of the peaks in the longitudinal conductivity[24] $\sigma_{xx}(B)$ of sample A to identify the QH tran-

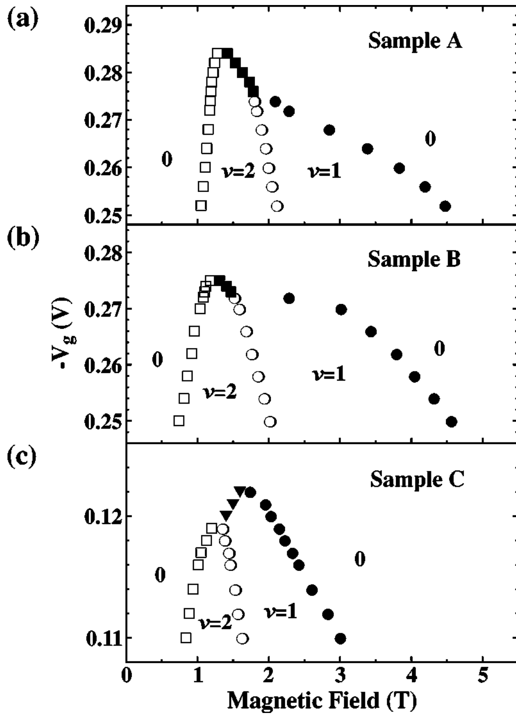

FIG. 7. (a)–(c) The phase diagrams of samples A,B, and C, obtained from the temperature independent behavior of $\rho_{xx}(B)$. The transitions between different quantum Hall liquids are 0-2 (open squares), 2-0 (solid squares), 2-1 (open circles), 1-0 (solid circles), and 0-1 (solid triangles).

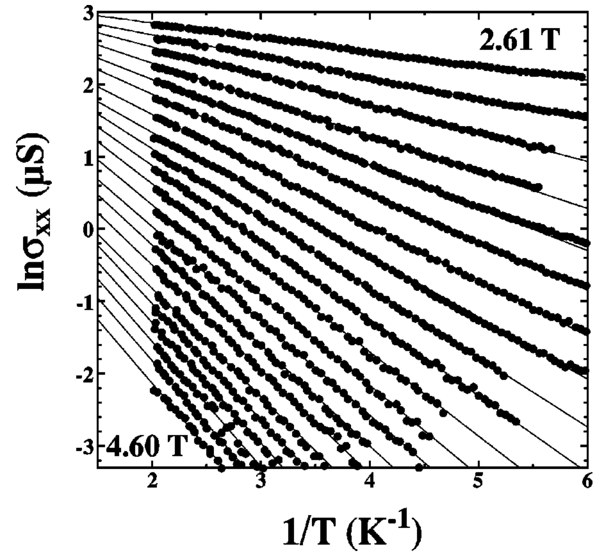

FIG. 8. Activation plots of the longitudinal conductivity σ_{xx} for sample B at filling factor $\nu=1$, at magnetic fields of 2.61, 2.28, 2.84, 3.00, 3.10, 3.20, 3.30, 3.40, 3.50, 3.60, 3.70, 3.80, 3.90, 4.00, 4.10, 4.20, 4.30, 4.37, 4.45, 4.52, and 4.60 T.

sitions, as described in Ref. 25. Using this other technique a phase diagram similar to Fig. 7(a) was obtained, confirming that in our samples temperature is a legitimate method for constructing the phase diagrams.

The phase diagram of the dot sample (A), shown in Fig. 7(a), is in between the spin-degenerate case (0-2-0 transitions as in Ref. 5) and the diagram showing stronger spin splitting [Fig. 7(c)]. To obtain further information about the $\nu=1$ liquid we measured the temperature dependence of the conductivity $\sigma_{xx}(T)$ of sample B; this is shown in Fig. 8 for 21 different carrier densities, while maintaining the filling factor at $\nu=1$. The conductivity shows activated behavior $\sigma_{xx}(T) \sim \exp(-\Delta_s/2k_BT)$ over the temperature range 0.15–0.5 K, and Fig. 9 shows the activation energy Δ_s determined from a least-squares fit to the data in Fig. 8. In sample B the spin gap Δ_s drops linearly to zero at a critical magnetic field $B_c=2.3$ T; similar measurements of Δ_s for sample C [see Fig. 9(b)] show more scatter, with the gap collapsing at $B_c \approx 1.9$ T. As shown in Fig. 3, the mobility of sample C is always greater than sample B, and the reduced value of B_c in sample C is consistent with there being less disorder. The spin gap Δ_s is expected to have the form

$$\Delta_s=2g_0\mu_BSB+E_{ex}=2g^*\mu_BSB, \tag{1}$$

where E_{ex} is the many-body exchange energy that lifts the g factor from its bare value ($g_o=0.44$) to its enhanced value g^*. An exchange enhancement by as much as 20 has been measured[26,27] in high-mobility GaAs 2DEG's. The measurements in Fig. 9 show that in the moderate-mobility InAs/GaAs samples the measured gap is enhanced over the single-particle Zeeman energy by a factor of 10, giving $g^*=5.5$; moreover, the exchange energy E_{ex} is roughly linear in B. The disorder broadening Γ_s can be calculated from the critical magnetic field, $\Gamma_s=\hbar/\tau_s=2g^*\mu_BSB_c$, and a lifetime $\tau_s=1.9$ ps is obtained, approximately agreeing with the quantum lifetime measured from Dingle plots. For magnetic fields where $\Delta_s<\Gamma_s$, the many-body interactions are destroyed by the disorder and only the bare Zeeman energy remains, and there is no spin splitting for magnetic fields less than the critical field B_c. In samples with more InAs, there is greater disorder, and the increased value of Γ_s pushes the critical field B_c higher. However, as discussed earlier the Zeeman splitting becomes more important at low carrier densities (and hence low magnetic fields). Both of these factors can explain why transitions to the $\nu=1$ liquid were not observed in earlier studies.[3–5]

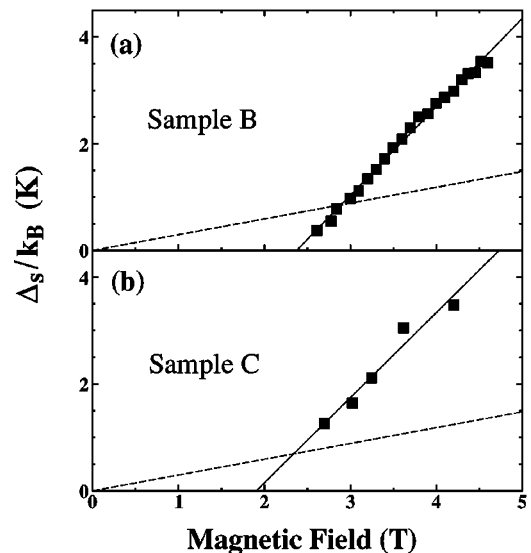

FIG. 9. The activation energy Δ_s for samples B and C, obtained from least-squares fits to the activated conductivity σ_{xx} at $\nu=1$. The dotted lines are the bare Zeeman energy assuming $|g_0|=0.44$.

The collapse of the spin splitting in the QH regime has been treated in mean-field theory by Fogler and Shklovskii,[28] who showed how disorder causes the spin gap to collapse at a critical filling factor ν_c. This theory has been applied to Shubnikov–de Haas measurements of high-mobility modulation-doped 2DEG's, see, for example, Refs. 29 and 30, where typically $\nu_c > 5$. The spin collapse measured in these InAs/GaAs systems occurs in the last LL ($\nu_c = 1$), and is caused by short-range scattering that is introduced by the InAs structures in the electron layer.

III. DISCUSSION

Transport measurements of both dash and dot samples (A–C) show insulator-QH transitions, whereas samples D and E do *not* show transitions. Likewise, samples processed from wafers A–C show Coulomb blockade oscillations in conductance measurements through a split gate, whereas samples D and E do not. We conclude that the repulsive short-range scattering introduced by the InAs dashes and dots provides the necessary disorder to observe the QH transitions at low n. In sample D there is a continuous monolayer of InAs deposited in the GaAs well, and no transitions between QH liquids or charging effects are measured; it is expected that the strain field emanating from the uniform InAs layer does not cause variations of the potential in the plane of the 2DEG.

Optical measurements at zero magnetic field show[31] that in a typical GaAs heterostructure the electrons in a 2DEG become localized into puddles about donor sites. With self-assembled structures, electron localization is more likely to occur in the vicinity of a InAs dash or dot, and indeed far-infrared measurements[32] of a sample similar to A show this to be the case. The Coulomb blockade characteristics in Figs. 4 and 5 show lateral tunneling through a quantum dot that is associated with a self-assembled InAs structure, and we speculate that the conduction band has the profile shown in Fig. 10. Lateral tunneling proceeds through the upper states, which are less strongly confined than the states within the InAs dot. We note that a similar strain modulation of the conduction band has been proposed by Tan *et al.*[33] to describe samples where a patterned $In_xGa_{1-x}As$ stressor layer was deposited 200 Å above a 2DEG. The picture presented in Fig. 10 is substantiated by an estimate of the dot diameter d, calculated from the self-capacitance of the dot ($C = 4\pi\epsilon\epsilon_0 d$) measured from the charging energy. From $e^2/C = 3$ meV, the dot diameter is estimated to be 370 Å, in rough agreement with TEM measurements.[17] Using these estimates, a puddle of electrons at an InAs dot site will contain approximately 10 electrons. This compares to other studies[34] where a much higher density of InAs dots was inserted into a 2DEG, and there were two electrons per InAs dot when the samples underwent a zero field metal-insulator transition.

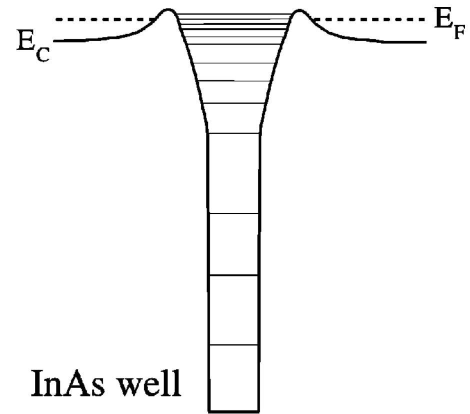

FIG. 10. Schematic diagram showing the bottom of the conduction band in the vicinity of an InAs dot. The deep InAs well is surrounded by barriers formed where the conduction band has been lifted by the strain field resulting from the 7% lattice mismatch between the InAs and GaAs.

IV. CONCLUSIONS

In conclusion, we have shown that by varying the amount of InAs deposited in the center of a GaAs quantum well, it is possible to control the spin splitting observed in the disorder–magnetic-field phase diagrams. The charging characteristics of individual quantum dots have been investigated, and samples that display Coulomb blockade oscillations also exhibit insulator–quantum Hall liquid transitions. Measurements of the spin gap at $\nu = 1$ shows its collapse at a critical magnetic field, the size of which correlates with the sample mobility. The two transport results, Coulomb blockade and quantum Hall transitions, can both be explained by assuming that the self-assembled InAs structures introduce repulsive scattering. For a given amount of InAs the scattering is stronger in dot samples than in dash samples; this is reflected both in mobility measurements, the degree of spin splitting observed in the n-B phase diagrams, and the associated spin gap Δ_s.

Our studies have established a link between the microscopic and macroscopic properties of a 2DEG that has been deliberately disordered, though we have not been able to detect significant differences between the dot and dash samples, an issue that requires further investigation.

We thank the Engineering and Physical Sciences Research Council (UK) for providing this work and one of the authors (J.T.N.) with financial support. D.A.R. acknowledges support from Toshiba Research Europe Ltd.

[1] D. Khmelnitskii, Phys. Lett. **106**A, 182 (1984).
[2] R.B. Laughlin, Phys. Rev. Lett. **52**, 2304 (1984).
[3] H.W. Jiang, C.E. Johnson, K.L. Wang, and S.T. Hannahs, Phys. Rev. Lett. **71**, 1439 (1993).
[4] T. Wang, K.P. Clark, G.F. Spencer, A.M. Mack, and W.P. Kirk, Phys. Rev. Lett. **72**, 709 (1994).
[5] R.J.F. Hughes, J.T. Nicholls, J.E.F. Frost, E.H. Linfield, M. Pepper, C.J.B. Ford, D.A. Ritchie, G.A.C. Jones, E. Kogan, and M. Kaveh, J. Phys.: Condens. Matter **6**, 4763 (1994).
[6] S.A. Kivelson, D.H. Lee, and S.C. Zhang, Phys. Rev. B **46**, 2223 (1992).
[7] D. Shahar, D.C. Tsui, and J.E. Cunningham, Phys. Rev. B **52**, 14

372 (1995).

[8] S.H. Song, D. Shahar, D.C. Tsui, Y.H. Xie, and D. Monroe, Phys. Rev. Lett. **78**, 2200 (1997).

[9] M. Hilke, D. Shahar, S.H. Song, D.C. Tsui, Y.H. Xie, and D. Monroe, Phys. Rev. B **56**, 15 545 (1997).

[10] S. das Sarma and A. Pinczuk, *Perspectives in Quantum Hall Effects* (Wiley, New York, 1997).

[11] H. Sakaki, G. Yusa, T. Someya, Y. Ohno, T. Noda, H. Akiyama, Y. Kadoya, and H. Noge, Appl. Phys. Lett. **67**, 3444 (1995).

[12] N. Horiguchi, T. Futatsugi, Y. Nakata, and N. Yokoyama, Appl. Phys. Lett. **70**, 2294 (1997).

[13] K. Yoh, J. Konda, S. Shiina, and N. Nishiguchi, Jpn. J. Appl. Phys., Part 1 **36**, 4134 (1997).

[14] E. Ribeiro, E. Muller, T. Heinzel, H. Auderset, K. Ensslin, G. Meideros-Ribeiro, and P.M. Petroff, Phys. Rev. B **58**, 1506 (1998).

[15] G. H. Kim, J. T. Nicholls, M. Pepper, and D. A. Ritchie, in *Proceedings of the 24th Conference on the Physics of Semiconductors, Jerusalem*, edited by D. Gershoni (World Scientific, Singapore, 1998).

[16] J.M. Garcia, G. Medeiros-Ribeiro, K. Schmidt, T. Ngo, J.L. Feng, A. Lorke, J. Kotthaus, and P.M. Petroff, Appl. Phys. Lett. **71**, 2014 (1997).

[17] G.D. Lian, J. Yuan, L.M. Brown, G.H. Kim, and D.A. Ritchie, Appl. Phys. Lett. **73**, 49 (1998).

[18] J. Yuan, G. D. Lian, G. H. Kim, D. A. Ritchie, Z. Y. Li, and L. M. Brown (unpublished).

[19] G.H. Kim, D.A. Ritchie, M. Pepper, G.D. Lian, J. Yuan, and L.M. Brown, Appl. Phys. Lett. **73**, 2468 (1998).

[20] We shall refer to the puddles of confined electrons also as dots, even though they may arise in structures containing InAs dashes.

[21] K.J. Thomas, J.T. Nicholls, N.J. Appleyard, M. Pepper, M.Y. Simmons, D.R. Mace, and D.A. Ritchie, Phys. Rev. B **58**, 4846 (1998).

[22] J.T. Nicholls, J.E.F. Frost, M. Pepper, D.A. Ritchie, M.P. Grimshaw, and G.A.C. Jones, Phys. Rev. B **48**, 8866 (1993).

[23] R.J. Haug, R.R. Gerhardts, K. von Klitzing, and K. Ploog, Phys. Rev. Lett. **59**, 1349 (1987).

[24] The conductivity $\sigma_{xx}=\rho_{xx}/(\rho_{xx}^2+\rho_{xy}^2)$ is calculated from the measured resistivities ρ_{xx} and ρ_{xy}.

[25] I. Glozman, C.E. Johnson, and H.W. Jiang, Phys. Rev. Lett. **74**, 594 (1995).

[26] R.J. Nicholas, R.J. Haug, K. von Klitzing, and G. Weimann, Phys. Rev. B **37**, 1294 (1988).

[27] A. Usher, R.J. Nicholas, J.J. Harris, and C.T. Foxon, Phys. Rev. B **41**, 1129 (1988).

[28] M.M. Fogler and B.I. Shklovskii, Phys. Rev. B **52**, 17 366 (1995).

[29] L.W. Wong, H.W. Jiang, E. Palm, and W.J. Schaff, Phys. Rev. B **55**, R7343 (1997).

[30] D.R. Leadley, R.J. Nicholas, J.J. Harris, and C.T. Foxon, Phys. Rev. B **58**, 13 036 (1998).

[31] G. Eytan, Y. Yayon, M. Rappaport, H. Shtrikman, and I. Bar-Joseph, Phys. Rev. Lett. **81**, 1666 (1998).

[32] S. Cinà, D.D. Arnone, H.P. Hughes, C.L. Foden, D. Whittaker, M. Pepper, and D.A. Ritchie, Phys. Rev. B **60**, 7780 (1999).

[33] I.H. Tan, R. Mirin, S. Shi, E. Hu, and J. Bowers, Appl. Phys. Lett. **61**, 300 (1992).

[34] E. Ribeiro, R. Jaggi, T. Heinzel, K. Ensslin, G. Meideros-Ribeiro, and P.M. Petroff, Phys. Rev. Lett. **82**, 996 (1999).